J. Iran. Chem. Soc., Vol. 6, No. 3, September 2009, pp. 620-637.

JOURNAL OF THE
Iranian
Chemical Society

Synthesis and Crystal Structure of Mn(II) and Hg(II) Compounds and Solution Studies of Mn(II), Zn(II), Cd(II) and Hg(II) Compounds Based on Piperazinediium Pyridine-2,3-dicarboxylate

H. Aghabozorg[a,*], S. Daneshvar[b], E. Motyeian[c], F. Manteghi[a], R. Khadivi[d], M. Ghadermazi[e], A. Shokrollahi[f], M. Ghaedi[f], S. Derki[f] and M. Shamsipur[g]

[a]*Faculty of Chemistry, Tarbiat Moallem University, Tehran, Iran*
[b]*Department of Chemistry, Islamic Azad University, Ardabil Branch, Ardabil, Iran*
[c]*Department of Chemistry, Faculty of Science, Payame Noor University, Qom Center, Qom, Iran*
[d]*Department of Chemistry, Islamic Azad University, North Tehran Branch, Tehran, Iran*
[e]*Department of Chemistry, Faculty of Science, University of Kurdistan, Sanandaj, Iran*
[f]*Department of Chemistry, Yasouj University, Yasouj, Iran*
[g]*Department of Chemistry, Razi University, Kermanshah, Iran*

(Received 18 August 2008, Accepted 26 September 2008)

Novel metal organic frameworks including $\{(pipzH_2)[Mn(py\text{-}2,3\text{-}dc)_2]\cdot 7.75H_2O\}_n$, **1**, $\{(pipzH_2)[Zn(py\text{-}2,3\text{-}dc)_2]\cdot 4H_2O\}_n$, **2**, $[Cd(py\text{-}2,3\text{-}dc)(H_2O)_3]_n$, **3** and $\{(pipzH_2)[Hg_4Cl_{10}]\}_n$, **4**, in which pipz is piperazine and py-2,3-dcH_2 is pyridine-2,3-dicarboxylic acid were synthesized applying a proton transfer ion pair *i.e.* $(pipzH_2)(py\text{-}2,3\text{-}dcH)_2$ and corresponding metallic salts and studied by IR, ^{1}H NMR, ^{13}C NMR spectroscopy and single crystal X-ray diffractometry. The space group of compounds **1** and **4** are $P2_1/c$ and $C2/c$ of monoclinic system, respectively. The crystal dimensions are a = 20.108(2) Å, b = 19.910(2) Å, c = 12.997(1) Å, β = 94.354(2)˚ for **1** and a = 15.940(1) Å, b = 11.2690(9) Å, c = 11.1307(9) Å, β = 90.685(2)˚ for **4**. The crystal structures of **2** and **3** have been reported previously. However, their solution studies are discussed here. The compounds had all polymeric structures. Although Zn^{II}, Cd^{II} and Hg^{II} were elements of the same group, their behavior against the ion pair was essentially different. Various supramolecular interactions mainly hydrogen bonds of the type O-H···O, N-H···O, C-H···O, N-H···Cl and C-H···Cl were observed in the structures. There was an unusual and huge water cluster in the structure of compound **1**. The solution states of compounds **1-4** were studied and reported. The protonation constants of pipz and py-2,3-dc, the py-2,3-dc/pipz proton transfer equilibrium constants and stoichiometry and stability of the system with Mn^{2+}, Zn^{2+}, Cd^{2+} and Hg^{2+} ions in aqueous solution were investigated by potentiometric *p*H titrations.

Keywords: Metal complexes, Crystal structure, Solution study, Supramolecular chemistry, Water cluster

INTRODUCTION

Crystal engineering based on metal organic frame works (MOFs) has recently attracted considerable interest, owing to their elegant framework topologies as well as their potential applications in molecular magnetism, catalysis, gas sorption, fluorescent sensing, and optoelectronic devices [1]. Studies in this field have focused on the design and preparation, as well

*Corresponding author. E-mail: aghabozorg@saba.tmu.ac.ir

as the structure-property relationships. Although big progress has been achieved [2], it is still a great challenge to predict the exact structures and composition of the assembly products built by coordination bonds and/or hydrogen bonds in crystal engineering. Research shows that there are several factors, such as the coordination nature of ligand structure, counter ions, *etc.*, which may act as a key for the rational design of MOFs. Therefore, systematic research on this topic is still warranted for understanding the roles of these factors in the formation of metal-organic coordination frameworks.

With respect to crystal engineering, the intrinsic geometric preferences of metal centers and various coordination sites of bridging ligands are the pivotal factors in determining the supramolecular architectures. Recent research has revealed that metal-directed self-assembly is one of the most useful strategies for generating intriguing metallosupramolecular architectures [3].

Starting with good proton donors and acceptors would result in supramolecular proton transfer compounds, and then using a rich variety of metal ions including *s*-, *p*-, *d*- and sometimes *f*-block metals, supramolecular metal complexes, namely metal organic frameworks could be built. In a brief review on about 140 structures, we have given the details about the synthesis, crystal structure, spectroscopy and solution studies of proton transfer ion pairs and their related metallic derivatives [4]. Accordingly, the remarkable significance of weak and strong interactions "beyond molecule" including hydrogen bonds, van der Waals forces, ion pairing and π-π interactions caused by different functional groups and their effects on explaining the structures is axiomatic [4].

An examination of our team work on the ion pair, $(pipzH_2)(py\text{-}2,3\text{-}dcH)_2$ [5], where pipz is piprazine and py-2,3-dcH_2 is pyridine-2,3-dicarboxylic acid, shows that the two polymeric compounds of Zn^{II}, **2** and Cd^{II}, **3** are derived from the ion pair [6,7]. Although in Zn^{II} compound, **2** both fragments of the ion pair are involved, in Cd^{II} compound, **3**, the cationic fragment *i.e.* piperazinediium ion has been lost.

In this paper, we intend to report the syntheses and crystal structures of two novel Mn^{II}, **1** and Hg^{II}, **4** compounds, derived from $(pipzH_2)(py\text{-}2,3\text{-}dcH)_2$. We would also like to discuss the solution behaviors of Mn^{II}, Zn^{II}, Cd^{II} and Hg^{II} compounds, **1**-**4**.

EXPERIMENTAL

General Methods and Materials

Manganese(II) sulfate monohydrate (99%), zinc(II) nitrate tetrahydrate (99%), cadmium(II) nitrate tetrahydrate (99%), mercury(II) chloride (99.5%), pyridine-2,3-dicarboxylic acid (97%), and piperazine (99%) were all purchased from Merck. The IR spectroscopy was performed applying a Perkin-Elmer 843 spectrophotometer (200-4000 cm^{-1}) using KBr disc. The NMR spectra were obtained on a Bruker DRX 500-Avance spectrometer, the chemical shifts are reported on the δ scale relative to TMS. The X-ray data were obtained with a Bruker SMART Diffractometer. Melting points were determined applying a Barnstead Electrothermal 9200 apparatus.

Single crystals of all the compounds suitable for crystallography were selected. Unit cell determination and data for the compounds were collected on a Bruker APEX II CCD area detector system [11,12] using Mo Kα radiation (λ = 0.71073 Å). The structures were solved and refined by full-matrix least-squares techniques on F^2 using SHELX-97 (SHELXL program package) [13,14]. The absorption corrections type was multi-scan. The hydrogen atoms of NH_2 groups and water molecules were found in different Fourier syntheses. The H(C) atom positions were calculated. All hydrogen atoms were refined in isotropic approximation in riding model with the U_{iso}(H) parameters equal to 1.2 $U_{eq}(C_i)$, 1.2 $U_{eq}(N_i)$ and 1.2 $U_{eq}(O_i)$, where $U(C_i)$, $U(N_i)$, $U(O_i)$ are respectively the equivalent thermal parameters of the carbon, nitrogen and oxygen atoms to which the corresponding H atoms are bonded. Refinement of F^2 was against all reflections. The weighted *R*-factor *wR* and goodness of fit S were based on F^2, conventional *R*-factors were based on *F*, with *F* set to zero for negative F^2. The threshold expression of $F^2 > 2\sigma(F^2)$ was used only for calculating *R*-factors(gt) *etc.*, and was not relevant to the choice of reflections for refinement. *R*-factors based on F^2 were statistically about twice as large as those based on *F*, and *R*-factors based on all data would be even larger.

A Model 794 Metrohm Basic Titrino was attached to an extension combined glass-calomel electrode mounted in an air-protected, sealed, thermostated jacketed cell maintained at 25.0 ± 0.1 °C by circulating water, from a constant-temperature bath (home-made thermostat), equipped with a

stirrer and a 10.000-ml-capacity Metrohm piston burette. The *p*H meter-electrode system was calibrated to read -log[H^+].

Synthesis of {$(pipzH_2)[Mn(py\text{-}2,3\text{-}dc)_2].7.75H_2O\}_n$, 1

Starting with aqueous solutions of 0.6 mmol (0.253 g) $(pipzH_2)(py\text{-}2,3\text{-}dcH)_2$, synthesized according to the literature [5], and 0.5 mmol (0.084 g) $MnSO_4.H_2O$, a lemon solution was obtained (Scheme 1). After 20 days yellow-orange crystals suitable for X-ray crystallography were settled at room temperature by slow evaporation. M.p.: 252 °C.

IR (KBr pellet): 3550-2400 (b, s), 1600 (sh, s), 1576 (sh, vs), 1443 (sh, m), 1380 (sh, vs), 1272 (sh, w), 1234 (sh, m), 1152 (sh, w), 1104 (sh, m), 876 (sh, m), 840 (sh, m), 708 (sh, m) cm^{-1}.

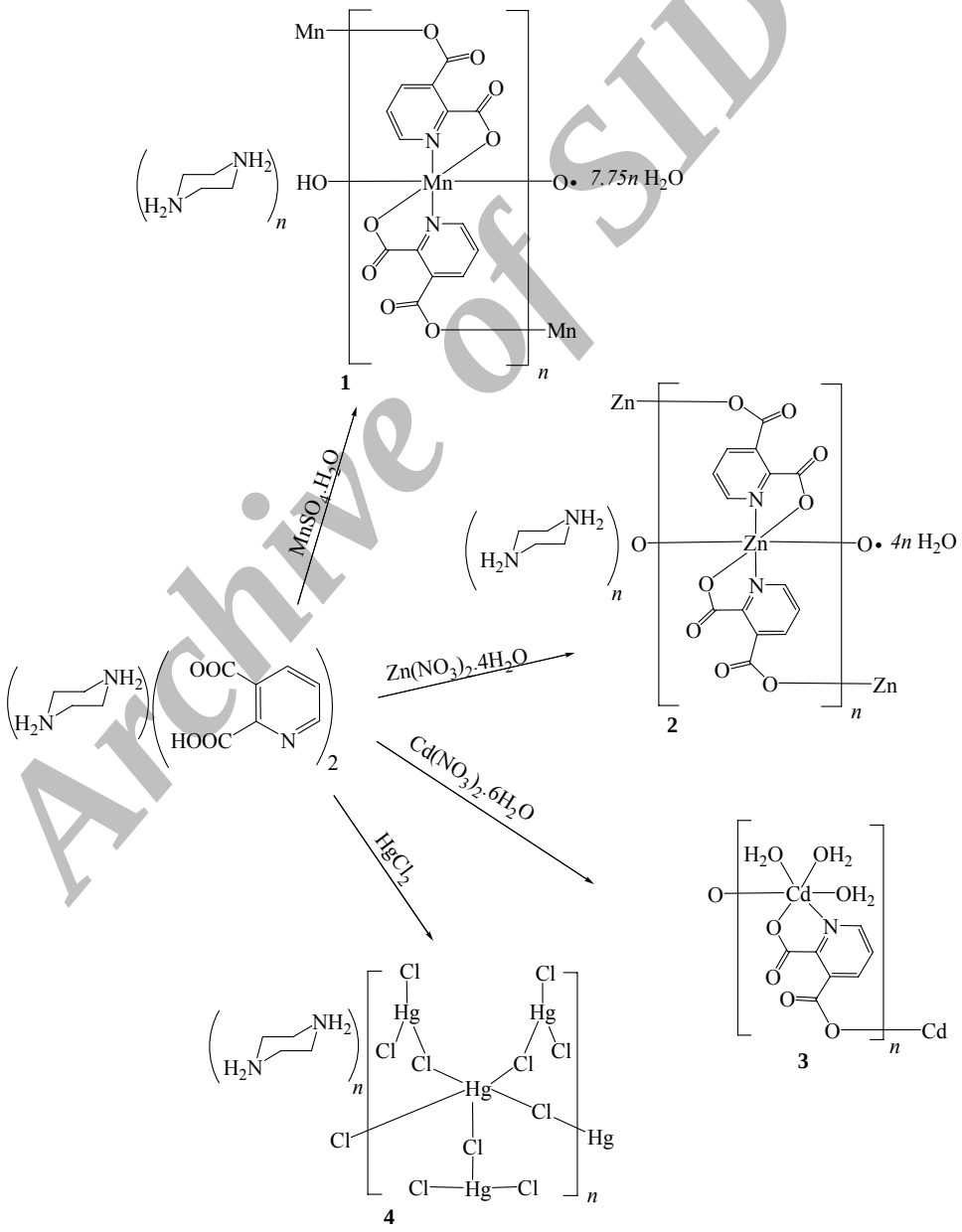

Scheme 1. Synthetic route to compounds **1-4**

Synthesis of $\{(pipzH_2)[Zn(py\text{-}2,3\text{-}dc)_2].4H_2O\}_n$, 2

A solution of 0.5 mmol (0.130 g) $Zn(NO_3)_2{\cdot}4H_2O$ in water (20 ml) was added to a solution of 0.60 mmol (0.253 g) of $(pipzH_2)(py\text{-}2,3\text{-}dc)_2$ [5] in water (20 ml) (Scheme 1). Colorless crystals were obtained by evaporation at room temperature after a few days [6].

Synthesis of $[Cd(py\text{-}2,3\text{-}dc)(H_2O)_3]_n$, 3

A solution of 0.5 mmol (0.158 g) $Cd(NO_3)_2{\cdot}4H_2O$ in water (20 ml) was added to a solution of 0.60 mmol (0.253 g) of $(pipzH_2)(py\text{-}2,3\text{-}dc)_2$ [5] in water (20 ml) (Scheme 1). Colorless crystals were obtained by evaporation at room temperature after a few days [7].

Synthesis of $\{(pipzH_2)[Hg_4Cl_{10}]\}_n$, 4

A solution of 1 mmol (0.271 g) $HgCl_2$ in water (20 ml) was added to a solution of 1.2 mmol (0.506 g) of $(pipzH_2)(py\text{-}2,3\text{-}dc)_2$ [5] in water (20 ml) (Scheme 1). By solvent evaporation at room temperature, colorless plate crystals of the title compound suitable for X-ray crystallography were obtained after a few weeks.

^{1}H NMR (DMSO-d_6): 1.13-3.90 (m, $pipzH_2$) ppm. ^{13}C NMR (DMSO-d_6): 38.2-39.9 (m, $pipzH_2$) ppm.

RESULTS AND DISCUSSION

A review of our team work on the ion pair, $(pipzH_2)(py\text{-}2,3\text{-}dcH)_2$ [5], reveals that two polymeric compounds of Zn^{II}, **2** and Cd^{II}, **3** have been derived from it [6,7], which are listed in Table 1. Although in Zn^{II} compound, **2** both fragments of the ion pair are involved, in Cd^{II} compound, **3**, the cationic fragment *i.e.* piperazinediium ion has been lost. A survey of the subject shows that Ni^{II} and two Cu^{II} compounds (Table 1) with an environment similar to Cd^{II} compound have been also reported [8-10]. For instance, from a high-dilution synthesis, crystals of $\{[Cu(py\text{-}2,3\text{-}dcH)_2]\}_n$ are obtained. The ligand pyridine-2,3-dicarboxylic acid ($py\text{-}2,3\text{-}dcH_2$) is a bidentate asymmetric molecule. The repeating units of this coordination polymer are metallacycles: two ligand molecules bridge two closest copper atoms in the chain. Each Cu^{II} atom has a distorted octahedral coordination sphere; the apical positions are occupied by the oxygen atoms of the non-deprotonated 3-carboxyl groups; the equatorial positions are occupied by two nitrogen atoms and two oxygen atoms of the deprotonated 2-carboxyl groups. This motif is a double chain.

X-ray Crystallographic Study of 1

The crystallographic data, selected bond lengths, bond angles, torsion angles and selected hydrogen bond geometries of $\{(pipzH_2)[Mn(py\text{-}2,3\text{-}dc)_2].7.75H_2O\}_n$, **1** are listed in Tables 2-4, respectively. Polymeric chains and coordination environment around Mn^{II} atoms, two illustrations of crystal packing and huge water cluster of compound **1** are shown in Figs. 1-4, respectively. As shown in Fig. 1, there are two different Mn^{II} atoms in the structure, each in the center of a parallel one dimensional chain. Mn1 is six-coordinated to O1 and N1 of one $(py\text{-}2,3\text{-}dc)^{2-}$ ring, O5 and N2 of second, O4 of third and O8 of fourth $(py\text{-}2,3\text{-}dc)^{2-}$ ring. Mn2 is also six-coordinated to O9 and N3 of one ring, O13 and N4 of second, O12 and O16 of two other rings. The coordination polyhedron around both Mn^{II} atoms is a distorted octahedral with O1-Mn1-O5 and O9-Mn2-O13 lying in axial positions with 15˚-16˚ deviation from linearity (Table 3). However, it can be seen in Figs. 2 and 3 that the polymeric structure is expanded

Table 1. Metallic Compounds Containing py-2,3-dc

Compound	Crystal system, Space group	Coordination geometry	Ref.
$\{(pipzH_2)[Zn(py\text{-}2,3\text{-}dc)_2]{\cdot}4H_2O\}_n$, **2**	Triclinic, $P\bar{1}$	Distorted octahedral	[6]
$[Cd(py\text{-}2,3\text{-}dc)(H_2O)_3]_n$, **3**	Orthorhombic, $Pca2_1$	Distorted octahedral	[7]
$[Ni(py\text{-}2,3\text{-}dc)(H_2O)_3]_n$	Monoclinic, $P2_1/c$	Distorted octahedral	[8]
$[Cu(py\text{-}2,3\text{-}dc)_2(H_2O)_2]$	Monoclinic, $P2_1/n$	Distorted octahedral	[9]
$[Cu(py\text{-}2,3\text{-}dcH)_2]_n$	Monoclinic, $P2_1/n$	Tetragonally elongated octahedral	[10]

Table 2. Crystallographic Data for Compounds **1**and **4**

	Mn^{II} compound, 1	Hg^{II} compound, 4
Empirical formula	$C_{144}H_{268}Mn_8N_{32}O_{126}$	$C_2H_6Cl_5Hg_2N$
Formula weight	4903.42	622.51
Temperature (K)	100(2)	100(2)
Wavelength (Å)	0.71073	0.71073
Crystal system	Monoclinic	Monoclinic
Space group	$P2_1/c$ $Z = 1$	$C2/c$ $Z = 8$
Unit cell dimensions	a = 20.108(2) Å	a = 15.940(1) Å
	b = 19.910(2) Å	b = 11.2690(9) Å
	c = 12.997(1) Å	c = 11.1307(9) Å
	β = 94.354(2)˚	β = 90.685(2)˚
Absorption coefficient (mm^{-1})	0.592	31.948
Min. and max. transmission factor	0.876, 0.901	0.051, 0.523
F(000)	2564	2160
Theta range for data collection	1.02 to 26.00˚	3.62 to 26.99˚
Index ranges	$-24 \le h \le 24$,	$-20 \le h \le 20$,
	$-24 \le k \le 24$,	$-14 \le k \le 14$,
	$-16 \le l \le 16$	$-14 \le l \le 14$
Reflections collected	43708	9964
Completeness to theta	99.9%	98.7%
	(to theta = 26.00˚)	(to theta = 26.99˚)
Refinement method	Full-matrix least-squares on F^2	Full-matrix least-squares on F^2
Data/restraints/parameters	10185/6/696	2120/0/101
Goodness-of-fit on F^2	1.04	1.00
Final R indices [I > 2sigma(I)]	$R1$ = 0.0547,	$R1$ = 0.030,
	w$R2$ = 0.149	w$R2$ = 0.077
Largest diff. peak and hole	1.016 and -0.500 e $Å^{-3}$	1.641 and -0.940 e $Å^{-3}$

Crystallographic data for the two structures have been deposited with the Cambridge Crystallographic Data Centre, CCDC 609886 for Mn^{II} compound and CCDC 609882 for Hg^{II} compound. Copies of the data can be obtained free of charge on application to the Director, CCDC, 12 Union Road, Cambridge CB2 1EZ, UK (Fax: int. code + (1223)336-033; e-mail for inquiry: fileserv@ccdc.cam.ac.uk; e-mail for deposition: deposit@ccdc.cam.ac.uk).

Table 3. Selected Bond Distances, Bond Angles and Torsion Angles (Å, ˚) for Compounds **1** and **4**

Compound **1**			
Mn1-O1	2.154 (3)	Mn2-O12	2.161 (3)
Mn1-O4^{i}	2.154 (3)	Mn2-O13^{iii}	2.161 (3)
Mn1-O5	2.177 (3)	Mn2-O9^{iv}	2.177 (3)
Mn1-O8^{ii}	2.164 (3)	Mn2-O16	2.169 (3)

Table 3. Continued

Mn1-N1	2.275 (4)	Mn2-N4iii	2.271 (4)
Mn1-N2	2.264 (4)	Mn2-N3^{iv}	2.278 (4)
O4^{i}-Mn1-O1	82.3 (1)	O12-Mn2-O13^{iii}	81.1 (1)
O4^{i}-Mn1-O8^{ii}	88.4 (1)	O12-Mn2-O16	89.7 (1)
O1-Mn1-O8^{ii}	108.5 (1)	O13^{iii}-Mn2-O16	110.8 (1)
O4^{i}-Mn1-O5	108.2 (1)	O12-Mn2-O9^{iv}	109.2 (1)
O1-Mn1-O5	164.9 (1)	O13^{iii}-Mn2-O9^{iv}	163.8 (1)
O8^{ii}-Mn1-O5	83.2 (1)	O16-Mn2-O9^{iv}	82.4 (1)
O^{iv}-Mn1-N2	93.3 (1)	O12-Mn2-N4^{iii}	154.3 (1)
O1-Mn1-N2	94.9 (1)	O13^{iii}-Mn2-N4^{iii}	74.0 (1)
O8^{i}-Mn1-N2	156.5 (1)	O16-Mn2-N4^{iii}	93.2 (1)
O5-Mn1-N2	74.0 (1)	O9^{iv}-Mn2-N4^{iii}	96.5 (1)
O4^{iv}-Mn1-N1	155.8 (1)	O12-Mn2-N3^{iv}	93.6 (1)
O1-Mn1-N1	74.0 (1)	O13^{iii}-Mn2-N3^{iv}	93.7 (1)
O8^{i}-Mn1-N1	94.9 (1)	O16-Mn2-N3^{iv}	155.5 (1)
O5-Mn1-N1	96.0 (1)	O9^{iv}-Mn2-N3^{iv}	73.6 (1)
N2-Mn1-N1	93.0 (1)	N4^{iii}-Mn2-N3^{iv}	94.3 (1)
O1-C1-C6-C2	177.1 (4)	O5-C8-C13-C9	178.1 (4)
O2-C1-C6-C2	-2.0 (6)	O6-C8-C13-C9	-1.9 (6)
O3-C2-C7-C1	-93.8 (5)	O7-C9-C14-C8	-91.3 (5)
O4-C2-C7-C1	90.6 (5)	O8-C9-C14-C8	93.4 (6)

Symmetry codes: *(i)* *x*, -*y*+1/2, *z*-1/2; (*ii*) *x*, -*y*+1/2, *z*+1/2; (*iii*) -*x*+2, -*y*+1, -*z*; (*iv*) -*x*+2, -*y*+1, -*z*+1.

Compound **4**			
Hg1-Cl2	2.304 (2)	Hg2-Cl4	2.76 (2)
Hg1-Cl1	2.307 (2)	Hg2-Cl4^{i}	2.87 (2)
Hg1-Cl3	2.980 (2)	Hg3-Cl6	2.290 (2)
Hg2-Cl3	2.427 (2)	Hg3-Cl5	2.930 (4)
Hg2-Cl5	2.528 (4)		
Cl2-Hg1-Cl1	172.92 (8)	Cl3^{ii}-Hg2-Cl4^{i}	93.5 (3)
Cl2-Hg1-Cl3	93.41 (7)	Cl5-Hg2-Cl4^{i}	80.5 (4)
Cl1-Hg1-Cl3	91.97 (8)	Cl4-Hg2-Cl4^{i}	7.9 (5)
Cl3^{ii}-Hg2-Cl3	130.4 (1)	Cl4^{ii}-Hg2-Cl4^{i}	163.9 (3)
Cl3^{ii}-Hg2-Cl5	120.9 (1)	Cl3^{ii}-Hg2-Cl4^{iii}	90.3 (5)
Cl3-Hg2-Cl5	108.5 (1)	Cl5-Hg2-Cl4^{iii}	90.5 (4)
Cl5-Hg2-Cl5^{ii}	15.7 (2)	Cl5^{ii}-Hg2-Cl4^{iii}	80.5 (4)
Cl3^{ii}-Hg2-Cl4	100.5 (3)	Cl4^{i}-Hg2-Cl4^{iii}	170.9 (8)
Cl3-Hg2-Cl4	88.5 (5)	Cl6^{ii}-Hg3-Cl6	177.6 (1)
Cl5-Hg2-Cl4	73.8 (4)	Cl6-Hg3-Cl5ii	93.2 (1)
Cl5ii-Hg2-Cl4	84.9 (4)	Cl6-Hg3-Cl5	84.4 (1)
Cl3-Hg2-Cl4i	90.3 (5)	Cl5ii-Hg3-Cl5	3.6 (1)
Cl4-Hg2-Cl4ii	158.5 (8)		
Cl4iii-Hg2-Cl4-Hg2i	-159 (5)	Cl4i-Hg2-Cl4-Hg2i	0.00 (5)
Cl4iii-Hg2-Cl4-Cl4i	-159 (5)	Cl5ii-Hg2-Cl5-Hg3	0.000 (3)
Cl4ii-Hg2-Cl3-Hg1	166.6 (5)	Cl5ii-Hg3-Cl5-Hg2	0.000 (3)
Cl4iii-Hg2-Cl3-Hg1	163.0 (5)		

Symmetry codes: (*i*) -*x*+1, -*y*+3, -*z*; (*ii*) -*x*+1, *y*, -*z*+1/2; (*iii*) *x*, -*y*+3, *z*+1/2.

Table 4. Selected Hydrogen Bond Geometry (Å, °) of Compound **1** and **4**

D-H···A	d(D-H)	d(H···A)	d(D···A)	<(D-H···A)
Compound **1**				
O1S-H1SB···O11	0.85	2.06	2.905 (5)	173
N6-H6B···O13S^{i}	0.92	1.87	2.785 (5)	173
O4S-H4SB···O1S	0.85	1.83	2.672 (5)	172
O5S-H5SB···O7S	0.85	1.87	2.717 (4)	174
O5S-H5SA···O7^{ii}	0.85	1.94	2.783 (5)	171
O10S-H10C···O1WA^{iii}	0.85	1.79	2.631 (7)	169
O10S-H10D···O6	0.85	1.80	2.641 (4)	171
O8S-H8SB···O5S	0.85	1.79	2.633 (5)	171
O13S-H13C···O2S^{iv}	0.85	2.04	2.890 (5)	180
O13S-H13D···O2^{v}	0.85	1.80	2.640 (4)	170
O6S-H6SA···O11^{vi}	0.85	1.89	2.737 (5)	175
O9S-H9SB···O10^{vi}	0.85	1.80	2.649 (4)	174
C5-H5A···O2WA	0.95	2.53	3.415 (8)	155
C17-H17A···O4S	0.95	2.57	3.520 (6)	176
C29-H29B···O11S^{vii}	0.99	2.35	3.196 (6)	143
C31-H31A···O6S^{vi}	0.99	2.36	3.225 (5)	146
Symmetry codes: (*i*) *x*+1, -*y*+1/2, *z*+1/2; (*ii*) -*x*+2, -*y*, -*z*; (*iii*) *x*, -*y*+1/2, *z*-1/2; (*iv*) *x*, -*y*+1/2, *z*+1/2; (*v*) *x*-1, *y*, *z*; (*vi*) *x*, -*y*+1/2, *z*-1/2; *(vii)* -*x*+2, -*y*, -*z*+1.				
Compound **4**				
N1S-H1B···Cl1^{i}	0.9	2.76	3.27 (1)	117
N1S-H1B···Cl6^{ii}	0.9	2.72	3.36 (1)	129
C1S-H1SA···Cl3^{iii}	0.97	2.32	3.15 (1)	143
C1S-H1SB···Cl1^{i}	0.97	2.7	3.36 (1)	126
C1S-H1SB···Cl4^{iv}	0.97	2.75	3.34 (2)	120
C1S-H1SB···Cl5^{iv}	0.97	2.64	3.48 (1)	144
Symmetry codes: (*i*) *x*-1/2, *y*-1/2, *z*; (*ii*) -x+1/2, *y*+1/2, -*z*+1/2; *(iii)* -*x*+1/2, *y*-1/2, -*z*+1/2; *(iv)* -*x*+1/2, -*y*+5/2, -*z*.				

through coordination of (py-2,3-dc)$^{2-}$ groups to Mn^{II} atoms, while (pipzH$_2$)$^{2+}$ ions and water molecules are located between the tapes of polymeric chains. Due to the large number of water molecules present and hydrogen bonds between them, there is a huge water cluster namely $(H_2O)_n$, $n = \infty$ with O···H distances of 1.79 to 2.57 Å given in Table 4 and illustrated in Fig. 4. As tabulated in Table 4, different O-H···O, N-H···O and C-H···O hydrogen bonds are formed between the fragments of the structure.

X-Ray Crystallographic Study of 4

The crystal data, selected bond lengths and angles, and selected hydrogen bonds geometry of $\{(pipzH_2)[Hg_4Cl_{10}]\}_n$, **4** are given in Tables 2-4, respectively. The molecular structure of the compound, coordination environment of three Hg^{II} atoms and crystal packing are illustrated in Figs. 5-7, respectively.

The compound **4** has an unusual structure. Compared with the compounds of Zn^{II}, **2** [6] and Cd^{II}, **3** [7], the title

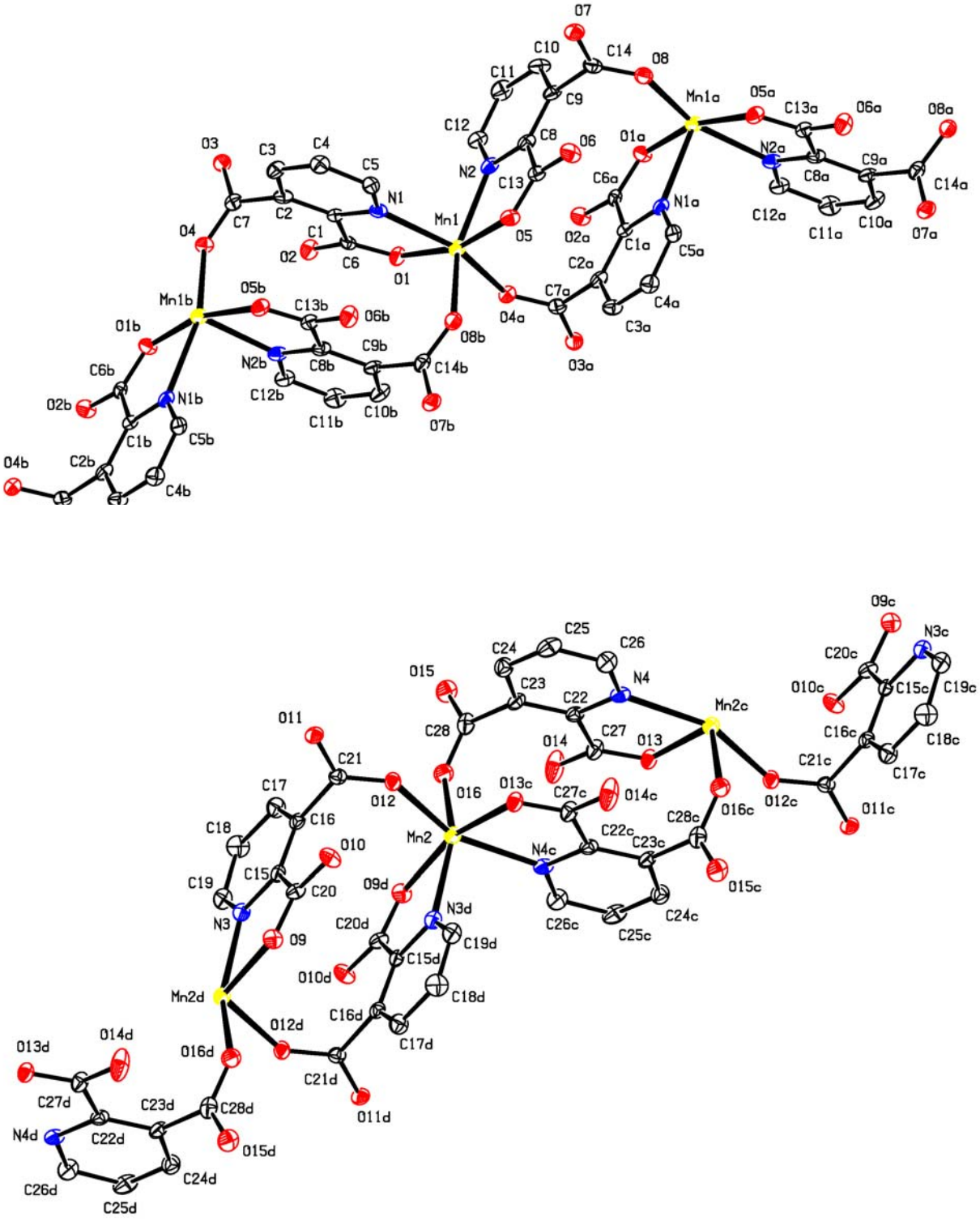

Fig. 1. Part of two polymeric chains of Mn^{II} compound, **1** containing Mn1 and Mn2 coordination environment in thermal ellipsoid representation with atom labeling. Hydrogen atoms are omitted for clarity.

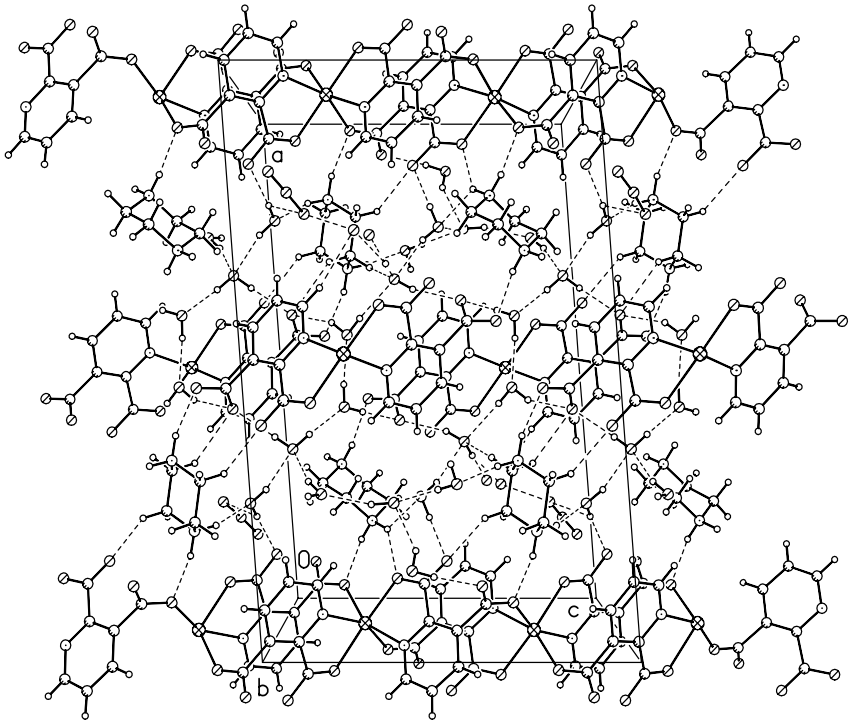

Fig. 2. Packing diagram of Mn^{II} compound, **1**, view along *b* axis. Hydrogen bonds are shown as dashed lines.

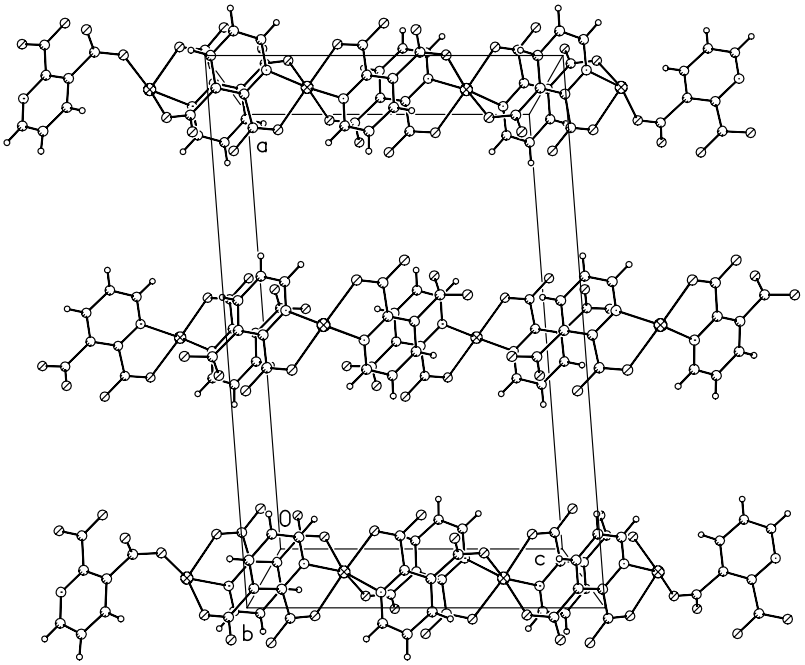

Fig. 3. Packing diagram of Mn^{II} compound, **1**, view along *b* axis showing only parallel chains of anionic fragments.

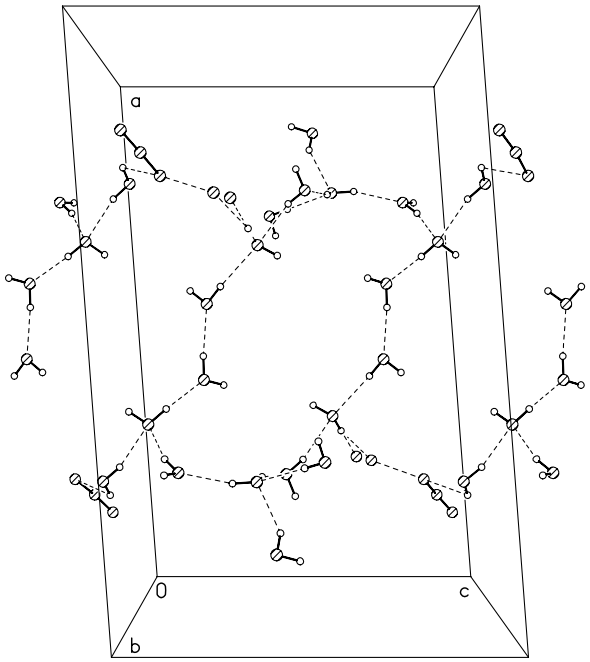

Fig. 4. The huge water cluster found in the unit cell of Mn^{II} compound, **1**, view along *b* axis.

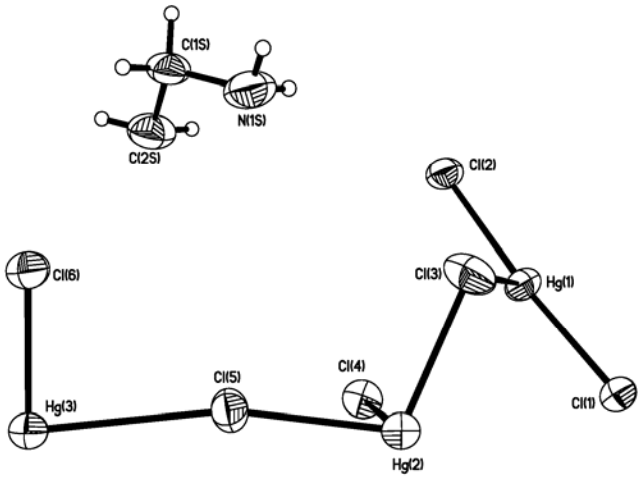

Fig. 5. Independent part of unit cell in $\{(pipzH_2)[Hg_4Cl_{10}]\}_n$ including one half of piperazinediium and a part of $[Hg_4Cl_{10}]$ fragments shown with 50% probability level.

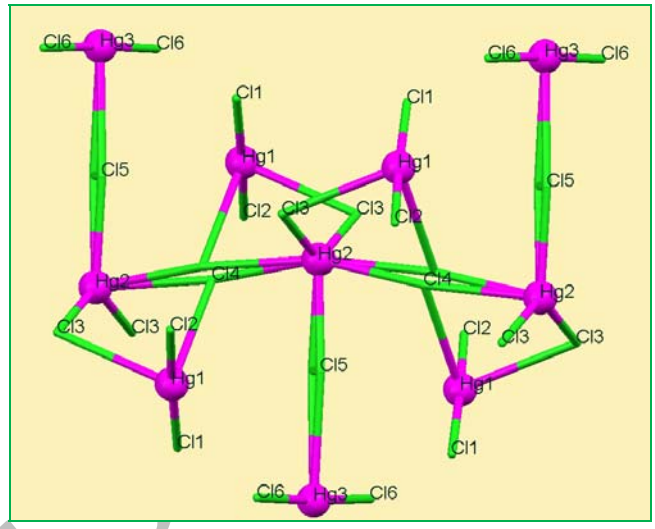

Fig. 6. Different coordination environment of three Hg^{II} atoms in repeating unit of Hg-Cl network of $\{(pipzH_2)[Hg_4Cl_{10}]\}_n$, piperazinediium species are omitted for clarity.

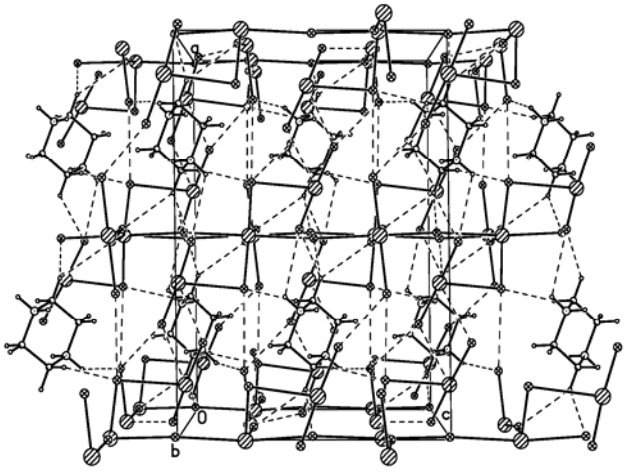

Fig. 7. Crystal packing fragment along *b* crystal axis of $\{(pipzH_2)[Hg_4Cl_{10}]\}_n$.

compound has an essentially different structure. In polymeric compound **2**, two $(py\text{-}2,3\text{-}dc)^{2-}$ fragments are coordinated to Zn^{II} and piperazinediium is incorporated in the structure as counter ion, as shown in Scheme 1. However, in polymeric compound **3** the piperazinediium is lost and Cd^{II} is coordinated by one $(py\text{-}2,3\text{-}dc)^{2-}$ and three water molecules, as given in Scheme 1. With regard to compound **4**, as is shown in Fig. 5, an infinite network of mercury and chlorine atoms is formed,

which is balanced by piperazinediium species. Two atoms *i.e.* Hg2 and Hg3 are situated in special positions and two chlorine atoms (Cl4 and Cl5) are disordered. This means that although they are depicted as whole atoms, they are only 1/2 as independent. In effect, Hg2 and Hg3 atoms lie on C2 axes that is parallel to *b* crystal axes and has [0.5, y, 0.25] coordinates. There are three types of Hg^{II} atoms in the Hg-Cl network that are well illustrated in Fig. 6. The chain of mercury and chlorine atoms can be expanded in one dimension containing Hg2 and Cl4 as the main chain and other Hg and Cl atoms as hanging groups (Fig. 6 and Scheme 1). The weak hydrogen bonds used for expanding the structure are of types N-H···Cl and C-H···Cl, as shown in Table 4 and crystal packing of Fig. 7.

Potentiometric Equilibrium Studies in Aqueous Solution

The details of such solution studies are described in previous works [15-20]. The concentrations of pipz and py-2,3-dcH_2 were 2.5 × 10^{-3} M, for the potentiometric *p*H titrations of py-2,3-dc, pipz and py-2,3-dc/pipz, in the absence and presence of 1.25 × 10^{-3} M metal ions. A standard carbonate-free NaOH solution (0.0983 M) was used in all titrations. The ionic strength was adjusted to 0.1 M with $NaNO_3$. Before an experimental point (*p*H) was measured, sufficient time was allowed for the establishment of equilibrium. Ligands' protonation constants and stability constants of proton transfer and their metal complexes were evaluated using the program described by Martell and Motekaitis [21]. The value of $K_w = [H^+][OH^-]$ was used in the calculations according to our previous works [15-20].

In preliminary experiments, the fully protonated forms of py-2,3-dc and pipz as the building blocks of the proton transfer system, were titrated with a standard NaOH aqueous solution (Figs. 8a and 8b, respectively), to obtain some information about their protonation constants. The protonation constants of py-2,3-dc and pipz were calculated by fitting the potentiometric *p*H data to the BEST program [21] whose results are summarized in Table 5. It is noteworthy that the resulting logβ values are in satisfactory agreement with those reported for py-2,3-dc [22], and pipz [23] in the literature. The determination of the equilibrium constants for the interactions between py-2,3-dc and pipz was accomplished through the comparison of the calculated and experimental *p*H profiles obtained with both py-2,3-dc and pipz present in a 1:1 ratio, as described before [15,24,25]. The results are shown in Table 6. The corresponding species distribution diagrams for py-2,3-dc/pipz are shown in Fig. 9. As is obvious, the most abundant proton-transfer species present at *p*H 8.1 (13.5%), 5.5 (22.2%) and 2.0 (50.1%) are pipzH/py-2,3-dc (logK = 1.84), pipzH_2py-2,3-dc (logK = 2.5) or pipzH/py-2,3-dcH (logK = 3.21), and pipzH_2/py-2,3-dcH_2 (logK = 2.99), respectively. The pipzH_2/py-2,3-dc, with the highest abundance of 50.1% at pH 2.0, is the only one in solution whose stichiometry supports

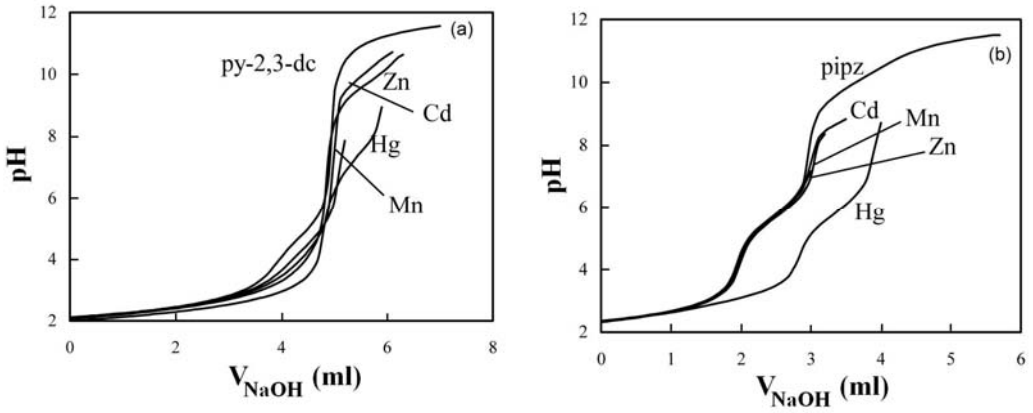

Fig. 8. Potentiometric titration curves for py-2,3-dc (a) and pipz (b) in the absence and presence of M^{2+} ions with NaOH 0.0983 M at 25 °C and μ = 0.1 M $NaNO_3$ M = Mn^{2+}, Zn^{2+}, Cd^{2+} and Hg^{2+}.

Table 5. Overall Stability Constants for Pipz/pydc/M^{2+}/H^{+} Binary and Ternary Systems at 25 °C and μ = 0.1 M KNO_3

System	m	l	q	h	logβ	Max %	at pH
pipz	0	0	1	1	9.91	98.00	8.0
	0	0	1	2	15.81	99.5	3.6
py-2,3-dc	0	1	0	1	5.19	91.3	3.9
	0	1	0	2	7.73	77.7	2.0
Mn-py-2,3-dc	1	1	0	0	3.45	30.2	>5.1
	1	1	0	2	10.06	26.4	2.0
	1	2	0	0	6.85	55.4	>7.9
	1	2	0	1	11.59	23.4	4.3
Zn-py-2,3-dc	1	1	0	1	14.68	51.2	2.5
	1	1	0	2	16.81	53.0	2.0
	1	2	0	0	15.82	99.4	6.9-7.5
	1	2	0	1	20.19	60.8	3.7
	1	2	0	2	22.60	12.4	2.6
	1	1	0	-1	-0.69	Negligible	-
	1	1	0	-2	-6.72	77.2	>11.0
	1	2	0	-1	1.53	Negligible	-
	1	2	0	-2	-4.24	22.6	>11.6
Cd-py-2,3-dc	1	1	0	0	8.95	10.2	5.1-9.0
	1	1	0	1	14.05	92.6	3.3
	1	1	0	2	16.04	49.2	2.0
	1	2	0	0	13.79	89.6	6.9-8.5
	1	2	0	2	18.34	Negligible	-
	1	1	0	-1	-3.83	Negligible	-
	1	1	0	-2	-9.77	70.0	>11.5
	1	2	0	-1	2.08	Negligible	-
	1	2	0	-2	-7.08	29.6	>11.5
Hg-py-2,3-dc	1	1	0	0	14.75	15.4	3.8
	1	1	0	1	17.48	36.2	2.0
	1	1	0	2	18.71	6.0	2.0
	1	2	0	0	19.59	86.8	6.4
	1	2	0	1	24.34	75.0	3.5
	1	2	0	2	26.42	27.6	2.0
	1	1	0	-2	1.18	99.8	9.2
Mn-pipz	1	0	1	0	4.67	3.2	7.0
	1	0	1	1	12.39	29.8	6.5
	1	0	2	0	8.30	Negligible	-
	1	0	2	1	15.62	Negligible	-
	1	0	1	-1	-1.22	96.2	8.1
	1	0	2	-1	1.83	43.6	>11.6

Table 5. Continued

Cd-pipz	1	0	1	1	11.87	16.6	7.3-7.8
	1	0	2	0	6.92	6.0	8.9
	1	0	2	1	15.30	2.6	8.5
	1	0	2	2	20.59	Negligible	-
	1	0	2	-1	-1.23	98.4	11.0
Hg-pipz	1	0	1	0	11.10	65.6	5.8
	1	0	2	0	17.79	97.0	9.8
	2	0	2	0	23.90	2.60	5.8
	2	0	2	1	30.20	37.6	4.0
	1	0	1	-1	1.44	15.4	11.9
Mn-py-2,3-dc-pipz	1	1	1	1	16.80	47.0	6.9
	1	1	1	3	24.14	Negligible	-
	1	1	1	4	30.32	76.0	2.0
	1	2	1	1	17.78	Negligible	-
	1	2	1	2	25.85	31.8	5.2
Zn-py-2,3-dc-pipz	1	1	1	1	16.31	Negligible	-
	1	1	1	2	23.14	Negligible	-
	1	1	1	3	25.76	Negligible	-
	1	1	1	4	35.69	45.6	2.0
	1	2	1	1	23.74	Negligible	-
	1	2	1	2	33.79	18.4	5.1
Cd-py-2,3-dc-pipz	1	1	1	1	18.72	Negligible	-
	1	1	1	2	29.38	78.2	4.3
	1	1	1	4	35.85	81.8	2.0
	1	2	1	1	25.88	21.4	8.2-8.6
Hg-py-2,3-dc-pipz	1	1	1	0	18.91	Negligible	-
	1	1	1	2	34.62	52.0	2.9
	1	1	1	4	39.30	67.0	2.0
	1	2	1	2	39.42	72.8	5.2
	1	1	2	0	27.54	57.0	9.4
	1	1	2	1	35.96	59.0	7.6
	1	1	2	2	42.62	27.4	6.5

the one evaluated from the solid state studies.

In order to evaluate the stoichiometry and stability of Mn^{II}, Zn^{II}, Cd^{II} and Hg^{II} compounds (**1-4**, respectively) with $pipzH_2$/py-2,3-dc association in aqueous solution, 2.5×10^{-3} M concentrations of py-2,3-dcH_2, pipz and their 1:1 mixture M were titrated with a 0.0983 M solution of NaOH at a temperature of 25 °C and an ionic strength of 0.1 M, maintained by $NaNO_3$, in the absence and presence of 1.25×10^{-3} M of metal ions. The resulting potentiometric *p*H titration curves are shown in Figs. 8 and 10. It was found that pipz forms very weak complexes with the Mn^{2+} and Cd^{2+} and no interaction with Zn^{2+}, while its interaction with Hg^{2+} is

Table 6. Overall Stability and Stepwise Recognition Constants for Interaction of pydc with pipz in 25 °C and μ = 0.1 M KNO_3

Stoichiometry			logβ	Equilibrium quotient K	logK	%max	at pH
Pipz	py-2,3-dc	h					
1	1	1	11.75	[pipzpydcH]/[pipzH][pydc]	1.84	13.5	8.1
1	1	2	18.31	$[pipzpydcH_2]/[pipzH][pydcH]$	3.21	22.2	5.5
				$[pipzpydcH_2]/[pipzH_2][pydc]$	2.50		
1	1	3	19.91	$[pipzpydcH_3]/[pipzH][pydcH_2]$	2.27	Negligible	-
1	1	4	26.53	$[pipzpydcH_4]/[pipzH_2][pydcH_2]$	2.99	50.1	2.0

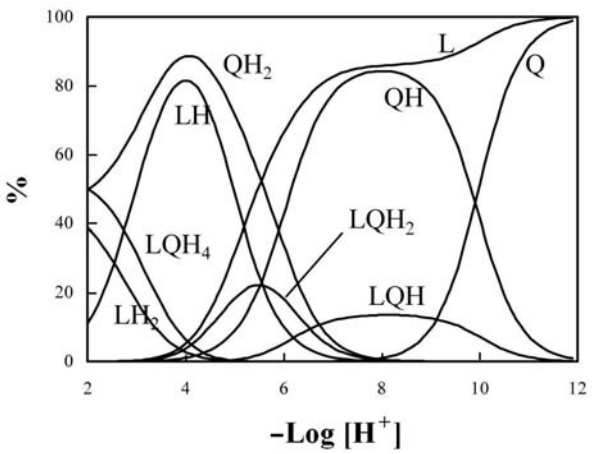

Fig. 9. Distribution diagram of proton transfer interaction between pipz (Q) and py-2,3-dc (L).

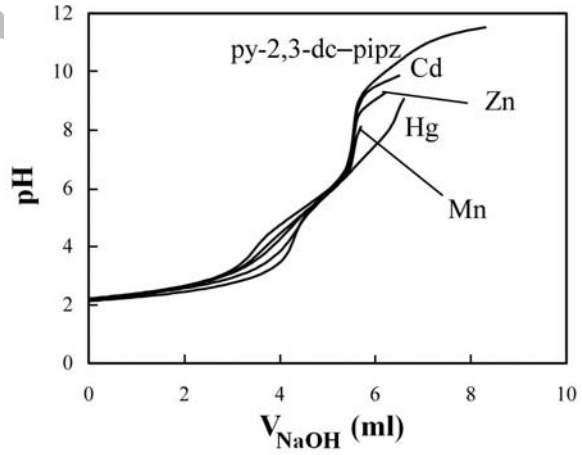

Fig. 10. Potentiometric titration curves for py-2,3-dc/pipz in the absence and presence of M^{n+} ions with NaOH 0.0983 M at 25 °C and μ = 0.1 M $NaNO_3$, M = Mn^{2+}, Zn^{2+}, Cd^{2+} and Hg^{2+}.

relatively strong. Meanwhile, the potentiometric titration curves of py-2,3-dc and py-2,3-dc/pipz mixture are depressed considerably in the presence of the metal ions, indicating the formation of more or less strong complexes with the metal ions used.

The extent of depression obviously depends both on the stoichiometries of resulting complexes and the ability of the metal ions to bind the ligand components. The cumulative stability constants, β_{mlqh}, are defined by Eq. (1) (charges are omitted for simplicity),

$$mM + lL + qQ + hH \rightleftharpoons M_mL_lQ_qH_h \qquad \beta_{mlqh}$$

$$\beta_{mlqh} = [M_mL_lQqH_h]/[M]^m[L]^l[Q]^q[H]^h \qquad (1)$$

where M is metal ion, L is py-2,3-dc, Q is pipz and H is proton, and m, l, q and h are the respective stoichiometric coefficients. Since the ligands' and complexes' activity coefficients are unknown, the β_{mlqh} values are defined in terms of concentrations.

The potentiometric *p*H titration curves of py-2,3-dc, pipz and their 1:1 mixture in the presence of metal ions were fitted to the BEST program [21], in order to evaluate the cumulative stability constants of the likely complex species in the solution. The corresponding distribution diagrams are shown in Figs. 11-13 with the results presented in Table 5. The data given in Table 5 revealed that Mn^{2+} and Cd^{2+} ions form relatively weak complexes with pipz alone, while the metal ions form much more stable complexes with py-2,3-dc and py-2,3-dc/pipz systems.

As it is obvious from Fig. 11 and Table 5, in the case of py-2,3-dc (L) and pipz (Q), as ligands , the most likely species with different metal ions are as follows:

(1) L = py-2,3-dc

Mn^{2+}: MnL, $MnLH_2$, MnL_2, and MnL_2H

Zn^{2+}: $ZnLH$, $ZnLH_2$, ZnL_2, ZnL_2H, ZnL_2H_2, $ZnLH_{-2}$ and ZnL_2H_{-2}

Cd^{2+}: CdL, $CdLH$, $CdLH_2$, CdL_2, $CdLH_{-2}$, and CdL_2H_{-2}

Hg^{2+}: HgL, $HgLH$, $HgLH_2$, HgL_2, HgL_2H_2, HgL_2H_{-2} and $HgLH_{-2}$.

(2) Q = pipz

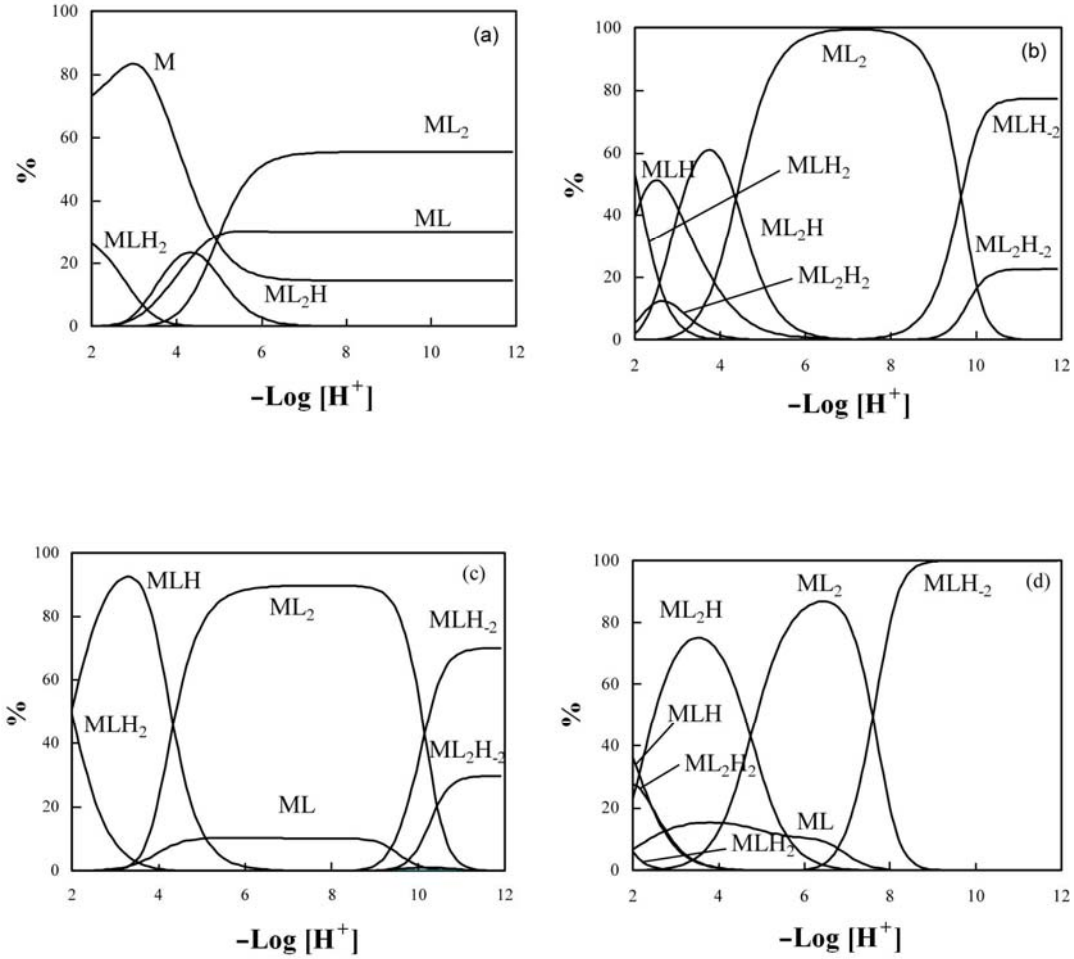

Fig. 11. Distribution diagrams of py-2,3-dc (L)/M binary systems. M = Mn^{2+} (a), Zn^{2+} (b), Cd^{2+} (c) and Hg^{2+} (d).

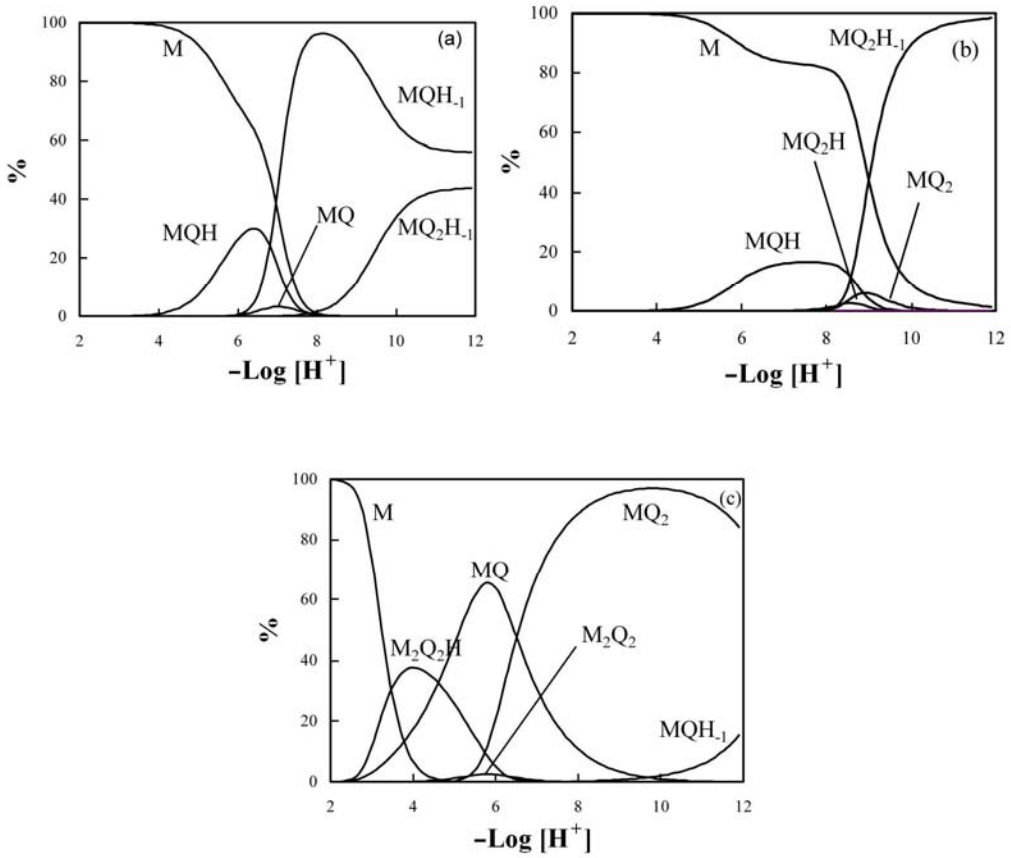

Fig. 12. Distribution diagrams of pipz/M binary systems. M = Mn^{2+} (a), Cd^{2+} (b) and Hg^{2+} (c).

Mn^{2+}: MnQ, MnQH, $MnQH_{-1}$ and MnQ_2H_{-1}

Cd^{2+}: CdQH, CdQ_2, CdQ_2H, and CdQ_2H_{-1}.

Hg^{2+}: HgQ, HgQ_2, Hg_2Q_2, Hg_2Q_2H and $HgQH_{-1}$.

As it is seen from Fig. 13 and Table 5, our solution studies carried out on the comlexation of different metal ions with the 1:1 py-2,3-dc (L)/pipz (Q) mixture revealed the formation of a variety of ternary complexes at different ranges of *p*H. The predominant species for different metal ions are as follows:

Mn^{2+}: MnLQH (at *p*H 6.9), $MnLQH_4$ (at *p*H 2.0), MnL_2QH_2 (at *p*H 5.2)

Zn^{2+}: $ZnLQH_4$ (at *p*H 2.0) and ZnL_2QH_2 (at *p*H 5.1)

Cd^{2+}: $CdLQH_2$ (at *p*H 4.3), $CdLQH_4$ (at *p*H 2.0), CdL_2QH (at *p*H 8.2-8.6)

Hg^{2+}: $HgLQH_2$ (at *p*H 2.9), $HgLQH_4$ (at *p*H 2.0), HgL_2QH_2 (at *p*H 5.2) $HgLQ_2$ (at *p*H 9.4), $HgLQ_2H$ (at *p*H 7.6) and $HgLQ_2H_2$ (at *p*H 6.5).

It is interesting to note that the stoichiometries of some of the most abundant ternary and binary complexes, existing in aqueous solution, including ZnL_2QH_2 (18.4% at *p*H 5.1), CdL (10.2% at *p*H 5.1-9.0), and MnL_2QH_2 (31.8% at *p*H 5.2) are very similar to those obtained for the corresponding isolated complexes in the solid state. However, for Hg^{2+} ion in solution, no significant ternary species in agreement with the isolated solid species was detected.

REFERENCES

[1] Y. Qi, F. Luo, Y. Che, J. Zheng, Cryst. Growth Des. 8 (2008) 606.

[2] a) C. Janiak, Dalton Trans. (2003) 2781; b) S.L. James, Chem. Soc. Rev. 32 (2003) 276; c) N.L. Rosi, J. Eckert, M. Eddaoudi, D.T. Vodak, J. Kim, M. O'Keeffe, O.M. Yaghi, Science 300 (2003) 1127.

[3] a) M. Fujita, M. Tominaga, A. Hori, B. Therrien, Acc.

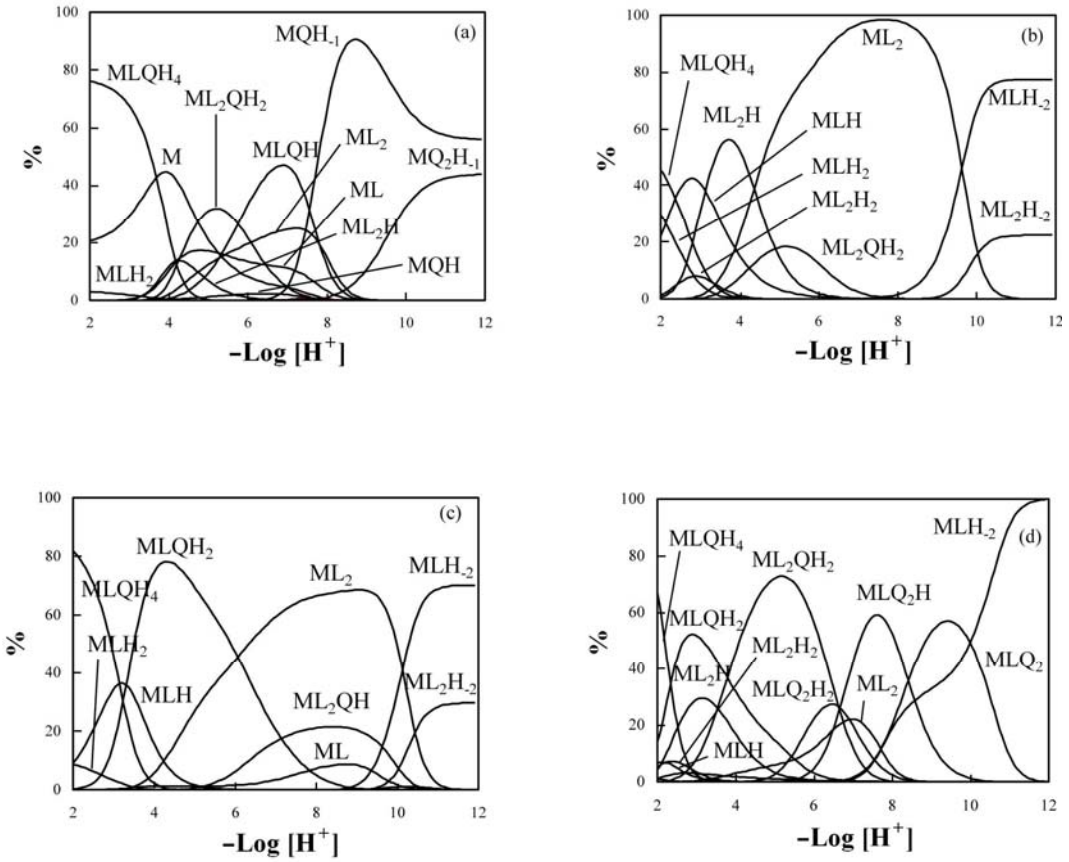

Fig. 13. Distribution diagrams of py-2,3-dc (L)/pipz (Q)/M ternary systems. M = Mn^{2+} (a), Zn^{2+} (b), Cd^{2+} (c) and Hg^{2+} (d).

Chem. Res. 38 (2005) 369; b) E. Menozzi, M. Busi, C. Massera, F. Ugozzoli, D. Zuccaccia, A. Macchioni, E.J. Dalcanale, J. Org. Chem. 71 (2006) 2617.

[4] H. Aghabozorg, F. Manteghi, S. Sheshmani, J. Iran. Chem. Soc. 5 (2008) 184, and references therein.

[5] H. Aghabozorg, F. Manteghi, M. Ghadermazi, Acta Crystallogr. E64 (2008) o230.

[6] H. Aghabozorg, S. Daneshvar, E. Motyeian, M. Ghadermazi, J. Attar Gharamaleki, Acta Crystallogr. E63 (2007) m2468.

[7] H. Aghabozorg, E. Motyeian, R. Khadivi, M. Ghadermazi, F. Manteghi, Acta Crystallogr. E64 (2008) m320.

[8] H. Yang, Z.-H. Zhang, J.-H. Guo, Y.-C. Lu, Jiegou Huaxue 25 (2006) 689.

[9] J.-F. Xiang, M. Li, S.-M. Wu, L.-J. Yuan, J.-T. Sun, Acta Crystallogr. E62 (2006) m1122.

[10] B.O. Patrick, C.L. Stevens, A. Storr, R.C. Thompson, Polyhedron 22 (2003) 3025.

[11] Bruker, SAINTPlus, v. 6.2. Data Reduction and Correction Program, Bruker AXS, Madison, Wisconsin, USA, 2001.

[12] Bruker, APEX2 software package, v. 1.27. Bruker Molecular Analysis Research Tool, Bruker AXS, Madison, Wisconsin, USA, 2005.

[13] G.M. Sheldrick, SADABS, v. 2.03, Bruker/Siemens Area Detector Absorption Correction Program, Bruker AXS, Madison, Wisconsin, USA, 2003.

[14] G.M. Sheldrick, SHELXTL, v. 6.12, Structure Determination Software Suite, Bruker AXS, Madison, Wisconsin, USA, 2001.

[15] A. Moghimi, V. Lippolis, H. Aghabozorg, A.

Shokrollahi, M. Shamsipur, S. Sheshmani, A.J. Blake, Polish J. Chem. 80 (2006) 1385.

[16] A. Moghimi, S. Sheshmani, A. Shokrollahi, M. Shamsipur, G. Kickelbik, H. Aghabozorg, Z. Anorg. Allg. Chem. 631 (2005) 160.

[17] H. Aghabozorg, F. Ramezanipour, J. Soleimannejad, M.A. Sharif, A. Shokrollahi, M. Shamsipur, A. Moghimi, J. Attar Gharamaleki, V. Lippolis, A.J. Blake, Polish J. Chem. 82 (2008) 487.

[18] A. Shokrollahi, M. Ghaedi, H. Ghaedi, J. Chin. Chem. Soc. 54 (2007) 933.

[19] A. Shokrollahi, M. Ghaedi, H.R. Rajabi, Ann. Chim. 97 (2007) 823.

[20] A. Shokrollahi, M. Ghaedi, M.S. Niband, H.R. Rajabi, J. Hazard. Mater. 151 (2008) 642.

[21] A.E. Martell, R.J. Motekaitis, Determination and Use of Stability Constants, 2nd ed., VCH, New York, 1992.

[22] J.S. Loring, M. Karlsson, W.R. Fawcett, W.H. Casey, Polyhedron 20 (2001) 1983.

[23] S. Cabani, V. Moilica, L. Lepori, S.T. Lobo, J. Phys. Chem. 81 (1977) 982.

[24] J.B. English Martell, A.E. Motekaitis, R.J. Murase, I. Inorg. Chim. Acta 258, 183 (1997).

[25] M.A. Sharif, H. Aghabozorg, A. Shokrollahi, G. Kickelbick, A. Moghimi, M. Shamsipur, Polish J. Chem. 80 (2006) 847.